

Water level changes at an ice-dammed lake in west Greenland inferred from InSAR data

M. Furuya¹ and J. M. Wahr

Cooperative Institute for Research in Environmental Sciences and Department of Physics, University of Colorado, Boulder, Colorado, USA

Received 10 May 2005; revised 2 June 2005; accepted 8 June 2005; published 16 July 2005.

[1] We detect ground displacements around an ice-dammed lake (Lake Tiningnilik) in west Greenland, using ERS1/2 and Envisat radar interferograms. We associate those displacements with draining episodes (jökulhlaups in Icelandic) that occurred in 1993 and 2003. We confirm those episodes in backscatter intensity images. By assuming a 7.5 meter/year increase in water level and using an elastic loading model, we predict a rate and spatial pattern for the deformation that are in good agreement with the observations. By generating digital elevation models from radar interferograms for both the drained and undrained stages, we validate the inferred lake level changes.

Citation: Furuya, M., and J. M. Wahr (2005), Water level changes at an ice-dammed lake in west Greenland inferred from InSAR data, *Geophys. Res. Lett.*, 32, L14501, doi:10.1029/2005GL023458.

1. Introduction

[2] Lake Tiningnilik is an ice-dammed lake (~ 30 km²) located south of the Jakobshaven ice fjord, Greenland (Figure 1). Although it is known that the lake drains at regular 10 year intervals [Braithwaite and Thomsen, 1984], there have been no systematic measurements of lake level variability due to a lack of convenient monitoring techniques. Outburst floods from ice-dammed lakes (jökulhlaups in Icelandic) are known to occur at a number of lakes in polar regions [e.g., Björnsson, 1998; Smith et al., 2000; Anderson et al., 2003]. For purposes of jökulhlaups hazard mitigation and a better understanding of jökulhlaups hydrodynamics [Roberts, 2005], it would be indispensable to quantitatively monitor the drainage and subsequent refilling of ice-dammed lakes. As is the case for many ice-dammed lakes, however, only scattered field observations are available for Lake Tiningnilik. We show that spaceborne synthetic aperture radar (SAR) data can be helpful in this regard.

[3] In this paper we provide an estimate of the rate of water level change in Lake Tiningnilik, based on ground displacements around the lake detected using ERS1/2 and Envisat radar interferograms. We assume those displacements are caused by water loading effects related to the 1993 and 2003 jökulhlaups (A. Weidick, personal communication). Radar backscatter intensity images confirm that draining episodes did occur at those times. Using elastic

load Green's functions to model the Earth's response to the changing water load, we use the observed ground displacements to estimate the water volume change during a draining episode. We validate that estimate by comparing digital elevation models (DEM) derived from ERS1/2 interferograms for drained and undrained times. This is the first systematic instrumental measurement of draining episodes at Lake Tiningnilik.

2. Data and Analysis Approach

[4] SAR is a remote sensing technique which allows us to continuously monitor the Earth's surface with fine spatial resolution regardless of weather [e.g., Curlander and McDonough, 1991; Cumming and Wong, 2005]. Through a measurement of phase values in SAR data at multiple acquisition dates, interferometric SAR (InSAR) enables us to form a DEM and, if the effects of topography are removed, to detect mm- to cm- ground displacements [Massonnet and Feigl, 1998; Rosen et al., 2000; Bürgmann et al., 2000; Hanssen, 2001]. The data source for this study is the European Space Agency's ERS1/2 and Envisat level-0 SAR data, from 1992 to 2004. We use a 250-meter resolution DEM provided by Kort and Matrikelstyrelsen, Denmark, to remove topographic fringes; its RMS error is estimated to be ~ 30 m [Ekholm, 1996]. Satellite state vectors are from the Technical University of Delft's precision orbit data [Scharroo and Visser, 1998]. The InSAR data processing was carried out using the Gamma commercial software package [Wegmüller and Werner, 1997].

[5] To quantitatively monitor lake level changes, we take the following approach. First, we identify draining episodes using SAR backscatter intensity images, and observe how the draining and undraining proceeded. The available DEM does not have the sufficient resolution or accuracy to match up with observed SAR surface features, so we cannot estimate the lake level directly from the intensity images. Instead we employ InSAR to detect loading displacements around the lake, and compare with model predictions to estimate the change in water volume. We use the ERS1/2 and Envisat SAR data archive to choose interferogram pairs that span the draining episodes and that have short perpendicular baselines to minimize DEM errors. Figure 2 shows the time spans covered by these pairs, superimposed on an idealized cartoon of the lake level that illustrates rapid draining during 1993 and 2003 followed by steady refilling. This cartoon is based on the conclusions of Braithwaite and Thomsen [1984], who used scattered lake level measurements during 1942–1983 to infer a drainage time constant of 0.24 years, and filling rates that varied by only about

¹On temporary leave from Earthquake Research Institute, University of Tokyo, Tokyo, Japan.

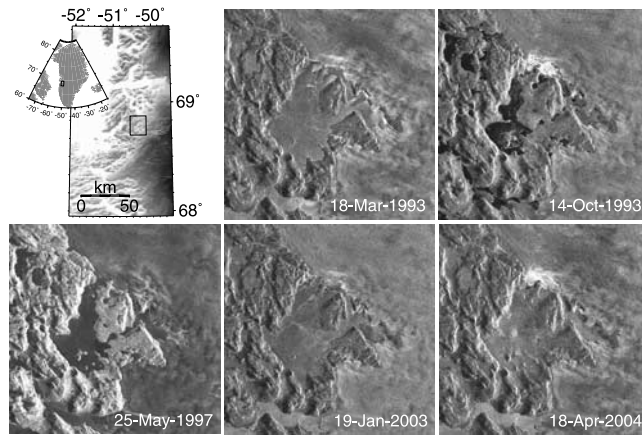


Figure 1. Location of Lake Tiningnilik in Greenland and SAR backscatter intensity images around the lake at five selected dates.

10%. from one year to another. Note that for each pair the first scene occurs immediately before a draining episode and the second scene occurs part way through the subsequent refilling period. Unfortunately, there are no short-baseline pairs spanning only the draining episode or only the refilling period.

[6] We validate our estimate of water volume change by using interferometric pairs that span short time intervals to construct DEM's both before and after the 1993 draining episode, and comparing the heights [see *Smith et al.*, 2000]. Other InSAR methods of estimating water levels have been used in previous studies (for a review, see *Smith* [2002]). For example, if there are persistently existing reflectors (e.g., leafless trees) sticking out of a water surface, interferograms can be formed even over the water that can result in cm-scale estimates of changes in water level [*Alsdorf et al.*, 2000, 2001; *Wdowinski et al.*, 2004]. Unfortunately, there are no such reflectors for Lake Tiningnilik.

3. Results and Discussion

3.1. Confirmation of Draining Episode Using Intensity Images

[7] Figure 1 shows SAR backscatter intensity images around Lake Tiningnilik at several times¹. The boundary between the lake and land is obscure in places, probably because of waves and/or frozen ice on the lake. However, we observe from these intensity images and intensity images at other times, that two draining episodes indeed took place during the past 12 years; one between March and October 1993 and the other between January 2003 and April 2004. This is consistent with independent field evidence that draining episodes occurred during the spring/summer of 1993 and of 2003. For instance, small islands in the lake are exposed in a drained period, but almost missing in an undrained period (Figure 1). Also, from images over the entire 12 year time period it is evident that the draining process is rapid while the filling

¹Auxiliary material is available at <ftp://ftp.agu.org/apend/gl/2005GL023458>.

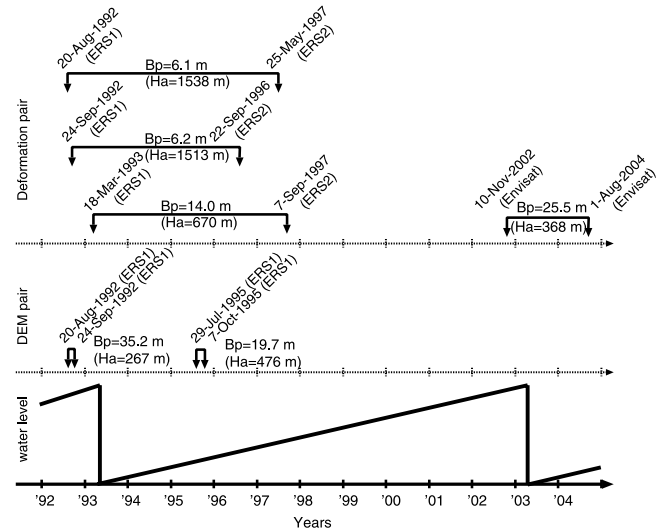


Figure 2. ERS1/2 and Envisat data for interferogram generation and a saw-tooth model for water level change.

process is slow, which supports the saw-tooth pattern shown in Figure 2 [*Braithwaite and Thomsen*, 1984]. The intensity images are therefore helpful in monitoring how much of the lake is filled with water, though they cannot provide a quantitative estimate of water volume as a function of time.

3.2. Detection of a Localized Unloading Deformation

[8] Each of the three independent interferograms in Figures 3a, 3b, and 3c shows shortening along the radar line of sight (LOS) near the lake. The spatial extent of the shortening signal is restricted to the region around the lake, which suggests its cause is also localized near the lake. The reason why the eastern half of Figure 3 has no deformation fields is that it undergoes temporal decorre-

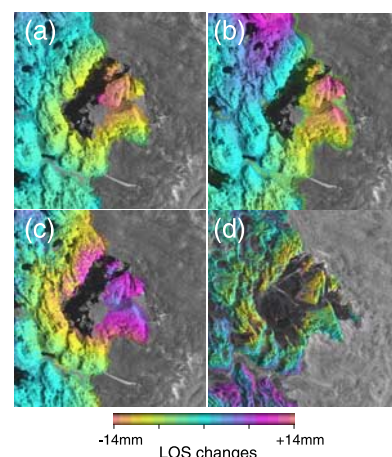


Figure 3. Differential interferograms. Data acquisition dates are (a) August 20, 1992, and May 25, 1997, (b) September 24, 1992, and September 22, 1996, (c) March 18, 1993, and September 7, 1997, and (d) November 10, 2002, and August 1, 2004. Light blue to yellow to red stands for a progressive shortening of the radar line of sight (LOS); one color cycle of LOS changes is 28 mm.

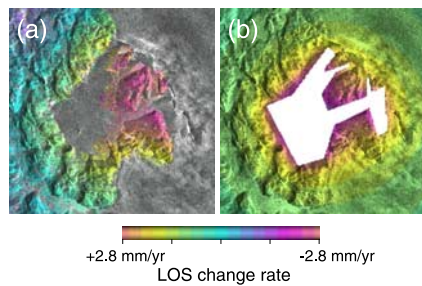


Figure 4. (a) Estimated deformation rate from the stacked radar interferograms, and (b) the predicted rate due to a water mass increase of 7.5 meter/year over the white region.

lation due to a presence of the Greenland ice sheet. The three interferograms span the 1993 draining episode, and thus we interpret them as uplift caused by the net removal of lake water during each time span. Since all three interferograms have short baselines (Figure 2) and the DEM has an RMS error of only up to ~ 30 m, it is unlikely that there are artifacts due to DEM errors. Since atmospheric signals tend to be temporally random, and since similar shortening signals are seen in each interferogram, it is also unlikely that the signals surrounding the lake are caused by atmospheric effects. Figure 3d is derived from the Envisat data pair, which spans the 2003 draining episode (see Figure 2). Although a shortening signal is also evident in this interferogram, and we believe it is the result of the 2003 event, the relatively long baseline length for this pair means that significant topographic errors are still a possibility. There are some prominent signals distal from the lake center in Figures 3b and 3d, which are presumably due to atmosphere.

[9] We stack the three ERS pairs, but omit the Envisat pair, to accentuate the signal and reduce atmospheric noise. In our stacking analysis we assume the time-dependence of the LOS lengthening at each point is proportional to the negative of the simple saw-tooth pattern shown in Figure 2, with the rationale that when the lake level rises (falls), the ground will subside (uplift). Specifically, we assume the LOS lengthening between any two times t_1 and t_2 , is $L = H(1 - (t_2 - t_1)/T)$, where H is the total lengthening occurring during the brief draining period, and T is the time (10 years) between draining events. We thus determine H by multiplying each interferogram by $T/(T - (t_2 - t_1))$, and finding the average of the three scaled interferograms. Figure 4a shows the results of this stacking, expressed as a mean loading deformation rate (H/T). The results clearly show a concentric phase change, with a maximum change in the LOS of 30 ± 5 mm, which is equivalent to a mean LOS lengthening rate of 3.0 ± 0.5 mm/year.

3.3. Water Volume Estimate Using an Elastic Loading Model

[10] We compare with the predictions of an elastic half-space loading model [Farrell, 1972], to estimate the total water level changes necessary to generate the observed displacements. We assume crustal values for the bulk and shear moduli of 5.2×10^{10} Pa and 2.6×10^{10} Pa, respectively [Shapiro and Ritzwoller, 2002]. Our predictions are relatively insensitive to these values. For exam-

ple, if the shear modulus is changed by 10%, which is probably close to its maximum uncertainty, the predicted displacement rates are affected at the 6% level, which is well below our InSAR uncertainty level. Figure 4b shows the predicted rate of LOS lengthening, computed assuming a 7.5 m/yr increase in water level uniformly distributed over the lake (i.e. the white region). Both the amplitude and concentric spatial pattern of the predicted displacement fields are in good agreement with the observed, supporting our hypothesis that the InSAR signal is caused by the lake load, and suggesting a lake filling rate of 7.5 m/yr. Since the filling time is 10 years, the total change, H , in water depth would be 75 m. Multiplying by the area of the lake, we find that the total water volume lost during the 1993 jökulhlaups was on the order of 2.3 km^3 . This is consistent with field-based estimates of $\sim 1.7 \text{ km}^3$ that characterized the 5 draining events occurring during 1945–1985 [Braithwaite and Thomsen, 1984].

3.4. Verification Using InSAR-Derived DEM

[11] To verify our InSAR estimate of the total lake level change, we generate DEMs using ERS1/2 data for short data spans (Figure 2), both before and after the 1993 draining event. A comparison of the two DEMs in Figures 5a and 5b shows the land surface area is wider in the drained stage (Figure 5b). Figures 5c and 5d show two profiles along each of the tracks X–Y and P–Q in Figures 5a and 5b, from which we can assess the change in lake level between 1992 and 1995. The change over this time interval should be about 70% of the total lake level change that occurred during the 1993 draining event.

[12] These two profiles are relatively free of contamination from layover and shadow effects. And the fact that solid and dashed results agree relatively well over common land points (i.e. over the regions close to X and Y

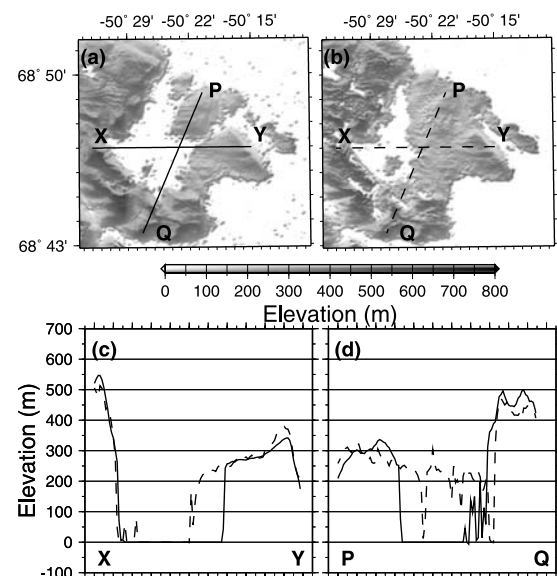


Figure 5. Estimated digital elevation models at (a) undrained, (b) drained times, and elevation profiles along (c) X–Y and (d) P–Q for both times. An elevation of zero means no data.

in (c), and close to P and Q in (d)) implies that misalignment errors are probably relatively small. Some care, though, is needed in interpreting the profiles. Since the water surface cannot maintain interferometric coherence over time, the height at water level cannot be estimated from InSAR data, and is set to zero. Thus, to estimate water level changes we must compare elevation values where they change abruptly from non-zero to zero. Around the middle of the X–Y profile in Figure 5c, the drained profile (dashed) changes from ~ 200 m to zero, while at a point somewhat closer to Y the undrained profile (solid) changes from ~ 260 m to zero, suggesting a ~ 60 m change in lake level during this period, and so a total lake level change of $\sim 60/0.70 = 85$ m during the draining event. Although the elevation profiles along P–Q (Figure 5d) are rather noisy, similar amplitudes are apparent. Therefore this independent analysis is consistent with our InSAR estimate of 75 meter water level changes.

[13] Note from Figures 5c and 5d that the land elevation profiles at identical points are not in exact agreement. Significant differences are evident, particularly at short scales. Typical differences at individual points are on the order of ~ 50 m, which can be interpreted as the error in these DEM estimates. As shown by Zebker *et al.* [1994], the error in the derived DEM is inversely proportional to the baseline separation. For these two interferograms the baselines (Figure 2) are rather short for an accurate DEM derivation. Atmospheric errors are also present. We thus did not use these InSAR-derived DEM's to attempt to further reduce the topographic fringes.

[14] **Acknowledgments.** We thank A. Weidick, C. E. Boggliid, E. Rignot and R. S. Anderson for providing us with information about the lake and jökulhlaups. The 250 meter resolution DEM was provided by S. Ekholm. We accessed ERS1/2 data under the Vectra consortium, and we acknowledge the coordinating efforts by A. Shepherd. Partial support was provided by a CIRES Visiting Fellowship and MEXT Japan (to M. Furuya) and by NASA grant NAG-12380. We thank D. Alsdorf and L. Smith for helpful reviews.

References

- Alsdorf, D., J. Melack, T. Dunne, L. Mertes, L. Hess, and L. Smith (2000), Interferometric radar measurements of water level changes on the Amazon floodplain, *Nature*, *404*, 174–177.
- Alsdorf, D., C. Birkett, T. Dunne, J. Melack, and L. Hess (2001), Water level changes in a large Amazon lake measured with spaceborne interferometry and altimetry, *Geophys. Res. Lett.*, *28*(14), L2671, doi:10.1029/2001GL012962.
- Anderson, S. P., J. S. Walder, R. S. Anderson, E. R. Kraal, M. Cunico, A. G. Fountain, and D. C. Trabant (2003), Integrated hydrologic and hydrochemical observations of Hidden Creek Lake jökulhlaups, Kennicott Glacier, Alaska, *J. Geophys. Res.*, *108*(F1), 6003, doi:10.1029/2002JF000004.
- Björnsson, H. (1998), Hydrological characteristics of the drainage system beneath a surging glacier, *Nature*, *395*, 771–774.
- Braithwaite, R. J., and H. H. Thomsen (1984), Runoff conditions at Kuusuaup Tasia, Christianshab, estimated by modeling, *Gletscher-Hydr. Meddelelser* *84*(2), 23 pp., Greenlands Geol. Underseegelse, Copenhagen.
- Bürgmann, R., P. A. Rosen, and E. J. Fielding (2000), Synthetic Aperture Radar interferometry to measure Earth's surface topography and its deformation, *Annu. Rev. Earth Planet. Sci.*, *28*, 169–209.
- Cumming, I. G., and F. H. Wong (2005), *Digital Processing of Synthetic Aperture Radar Data Algorithms and Implementation*, 625 pp., Artech House, Norwood, Mass.
- Curlander, J. C., and R. N. McDonough (1991), *Synthetic Aperture Radar Systems and Signal Processing*, 647 pp., John Wiley, Hoboken, N. J.
- Ekholm, S. (1996), A full coverage, high-resolution, topographic model of Greenland computed from a variety of digital elevation data, *J. Geophys. Res.*, *101*, 21,961–21,972.
- Farrell, W. E. (1972), Deformation of the Earth by surface loads, *Rev. Geophys.*, *10*, 761–797.
- Hanssen, R. F. (2001), *Radar Interferometry—Data Interpretation and Error Analysis*, 308 pp., Springer, New York.
- Massonnet, D., and K. L. Feigl (1998), Radar interferometry and its application to changes in the Earth's surface, *Rev. Geophys.*, *36*, 441–500.
- Roberts, M. J. (2005), Jkúlhláups: A reassessment of floodwater flow through glaciers, *Rev. Geophys.*, *43*, RG1002, doi:10.1029/2003RG000147.
- Rosen, P. A., S. Hensley, I. R. Joughin, F. K. Lin, S. N. Madsen, R. Rodriguez, and R. M. Goldstein (2000), Synthetic aperture radar interferometry—Invited paper, *Proc. IEEE*, *88*, 333–382.
- Scharroo, R., and P. Visser (1998), Precise orbit determination and gravity field improvement for the ERS satellites, *J. Geophys. Res.*, *103*, 8113–8127.
- Shapiro, N. M., and M. H. Ritzwoller (2002), Monte-Carlo inversion for a global shear velocity model of the crust and upper mantle, *Geophys. J. Int.*, *151*, 88–105.
- Smith, L. C. (2002), Emerging applications of interferometric synthetic aperture radar in geomorphology and hydrology, *Ann. Assoc. Am. Geog.*, *92*, 385–398.
- Smith, L. C., D. E. Alsdorf, F. J. Magilligan, B. Gomez, L. A. K. Mertes, N. D. Smith, and J. B. Garvin (2000), Estimates of erosion, deposition, and net volumetric change caused by the 1996 Skeidarársandur jökulhlaup, Iceland, from synthetic aperture radar interferometry, *Water Resour. Res.*, *36*, 1583–1594.
- Wdowinski, S., F. Amelung, F. Miralles-Wilhelm, T. H. Dixon, and R. Carande (2004), Space-based measurements of sheet-flow characteristics in the Everglades wetland Florida, *Geophys. Res. Lett.*, *31*, L15503, doi:10.1029/2004GL020383.
- Wegmüller, U., and C. L. Werner (1997), Gamma SAR processor and interferometry software, *Eur. Space Agency Spec. Publ.*, *ESA SP-414*, 1686–1692.
- Zebker, H. A., C. L. Werner, P. A. Rosen, and S. Hensley (1994), Accuracy of topographic maps derived from ERS-1 interferometric radar, *IEEE Trans. Geosci. Remote Sens.*, *32*, 823–836.

M. Furuya and J. M. Wahr, CIRES, University of Colorado, Boulder, CO 80309, USA. (masato@colorado.edu; furuya@eri.u-tokyo.ac.jp)